

Synthesis, Structure, and Solid-State Transformation Studies of Phosphonoacetate Based Hybrid Compounds of Uranium and Thorium

Padmini Ramaswamy, Ramanath Prabhu, and Srinivasan Natarajan*

Framework Solids Laboratory, Solid State and Structural Chemistry Unit,
Indian Institute of Science, Bangalore 560 012, India

Received May 24, 2010

Three new phosphonoacetate hybrid frameworks based on the actinide elements uranium and thorium have been synthesized. The compounds $[C_4N_2H_{14}][(UO_2)_2(O_3PCH_2COO)_2] \cdot H_2O$, **I**, $[C_4N_2H_{14}][(UO_2)_2(C_2O_4)(O_3PCH_2COOH)_2]$, **II**, and $Th(H_2O)_2(O_3PCH_2COO)(C_2O_4)_{0.5} \cdot H_2O$, **III**, are built up from the connectivity between the metal polyhedra and the phosphonoacetate/oxalate units. Compound **II** has been prepared using a solvent-free approach, by a solid state reaction at 150 °C. It has been shown that **II** can also be prepared through a room temperature mechanochemical (grinding) route. The layer arrangement in **III** closely resembles to that observed in **I**. The compounds have been characterized by powder X-ray diffraction, IR spectroscopy, thermogravimetric analysis, and fluorescence studies.

Introduction

Compounds based on actinides are beginning to attract the attention of synthetic chemists as they offer interesting possibilities because of their variable coordination abilities.¹ Uranium based compounds have been extensively investigated, and their coordination chemistry discussed in detail during the early 1960s by Evans et al.^{2a} and others.^{2b,c} The fascinating crystal chemistry of uranium continues to be the focus of intense research activity.³ The use of hydrothermal

conditions for the preparation of uranium compounds has been pursued vigorously, giving rise to a diverse variety of compounds.⁴ The advent of metal–organic framework compounds based on aromatic/aliphatic carboxylates have provided an added impetus to study the reactivity of the actinide group elements, especially uranium.⁵ Many actinide elements exhibit structures that are unique and act as model compounds in the area of mineralogy and mineral chemistry.⁶

Clearfield and co-workers have investigated in detail the reactivity of phosphonic acids using both the main group as well as the d-block elements.^{7–11} Both mono- as well as di-phosphonic acids with flexible carbon-chain backbones have been employed in the preparation of new phosphonate

*To whom correspondence should be addressed. E-mail: snatarajan@sscu.iisc.ernet.in.

(1) (a) Knope, K. E.; Cahill, C. L. *Inorg. Chem.* **2008**, *47*, 7660. (b) Alsobrook, A. N.; Albrecht-Schmitt, T. E. *Inorg. Chem.* **2009**, *48*, 11079. (c) Nelson, A.-G. D.; Bray, T. H.; Zhan, W.; Haire, R. G.; Saylor, T. S.; Albrecht-Schmitt, T. E. *Inorg. Chem.* **2008**, *47*, 4945. (d) Knope, K. E.; Cahill, C. L. *Inorg. Chem.* **2009**, *48*, 6845. (e) Ok, K. M.; Sung, J.; Hu, G.; Jacobs, R. M. J.; O'Hare, D. *J. Am. Chem. Soc.* **2008**, *130*, 3762. (f) Halasyamani, P. S.; Walker, S. M.; O'Hare, D. *J. Am. Chem. Soc.* **1999**, *121*, 7415. (g) Kim, J.-Y.; Norquist, A. J.; O'Hare, D. *Chem. Commun.* **2002**, 2198. (h) Francis, R. J.; Halasyamani, P. S.; O'Hare, D. *Chem. Mater.* **1998**, *10*, 3131. (i) Francis, R. J.; Halasyamani, P. S.; O'Hare, D. *Angew. Chem., Int. Ed.* **1998**, *37*, 2214. (j) Knope, K. E.; Cahill, C. L. *Eur. J. Inorg. Chem.* **2010**, 1177. (k) Adelani, P. O.; Albrecht-Schmitt, T. E. *Inorg. Chem.* **2010**, *49*, 5701.

(2) (a) Evans, H. T., Jr. *Science* **1963**, *141*, 154. (b) Penneman, R. A.; Asprey, L. B.; Sturgeon, G. *J. Am. Chem. Soc.* **1962**, *84*, 4608. (c) Sturgeon, G. D.; Penneman, R. A.; Kruse, F. H.; Asprey, L. B. *Inorg. Chem.* **1965**, *4*, 748.

(3) (a) Burns, P. C.; Miller, M. L.; Ewing, R. C. *Can. Mineral.* **1996**, *34*, 845. (b) Burns, P. C. *Rev. Mineral.* **1999**, *38*, 23. (c) Burns, P. C. *Can. Mineral.* **2005**, *43*, 1839.

(4) (a) Cahill, C. L.; Burns, P. C. *Inorg. Chem.* **2001**, *40*, 1347. (b) Li, Y.; Cahill, C. L.; Burns, P. C. *Chem. Mater.* **2001**, *13*, 4026. (c) Bean, A. C.; Campana, C. F.; Kwon, O.; Albrecht-Schmitt, T. E. *J. Am. Chem. Soc.* **2001**, *123*, 8806. (d) Francis, R. J.; Drewitt, M. J.; Halasyamani, P. S.; Ranganathachar, C.; O'Hare, D.; Clegg, W.; Teat, S. J. *Chem. Commun.* **1998**, *2*, 279.

(5) (a) Chen, W.; Hong, H.-M.; Wang, J.-Y.; Liu, Z.-Y.; Xu, J.-J.; Yang, M.; Chen, J.-S. *J. Am. Chem. Soc.* **2003**, *125*, 9266. (b) Yu, Z. T.; Liao, Z.-L.; Jiang, Y.-S.; Li, G.-H.; Chen, J.-S. *Chem.—Eur. J.* **2005**, *11*, 2642. (c) Frisch, M.; Cahill, C. L. *Dalton Trans.* **2006**, 39, 4679. (d) Frisch, M.; Cahill, C. L. *J. Solid State Chem.* **2007**, *180*, 2597. (e) Kim, J.-Y.; Norquist, A. J.; O'Hare, D. *J. Am. Chem. Soc.* **2003**, *125*, 12688.

(6) (a) Wang, S.; Alekseev, E. V.; Diwu, J.; Casey, W. H.; Phillips, B. L.; Depmeier, W.; Albrecht-Schmitt, T. E. *Angew. Chem., Int. Ed.* **2010**, *49*, 1057. (b) Mao, Y.; Baka, A. *Inorg. Chem.* **1996**, *35*, 3925. (c) Albrecht-Schmitt, T. E. *Angew. Chem., Int. Ed.* **2005**, *44*, 4836. (d) Krivovichev, S. V.; Kahlenberg, V.; Kaindl, R.; Mersdorf, E.; Tananaev, I. G.; Myasoedov, B. F. *Angew. Chem., Int. Ed.* **2005**, *44*, 1134.

(7) (a) Grohol, D.; Clearfield, A. *J. Am. Chem. Soc.* **1997**, *119*, 4662. (b) Martin, K. J.; Squartrito, P. J.; Clearfield, A. *Inorg. Chim. Acta* **1989**, *155*, 7. (c) Zhang, Y.; Clearfield, A. *Inorg. Chem.* **1992**, *31*, 2821. (d) Grohol, D.; Subramaniam, M. A.; Poojary, D. M.; Clearfield, A. *Inorg. Chem.* **1996**, *35*, 5264.

(8) Clearfield, A. *Curr. Opin. Solid State Mater. Sci.* **1996**, *1*, 268.
(9) Clearfield, A. *Curr. Opin. Solid State Mater. Sci.* **2002**, *6*, 495.
(10) Clearfield, A. *Chem. Mater.* **1998**, *10*, 2801.
(11) Clearfield, A. *Dalton Trans.* **2008**, 44, 6089.

solids. The phosphonate structures exhibit considerable variety and in a few cases are analogous to the phosphate structures.^{8–10,12–16} The replacement of one of the phosphonic acid groups in a diphosphonic acid by a carboxylic acid group gives rise to phosphonocarboxylic acids. The use of two different functional groups, along with the availability of a flexible carbon backbone is attractive as they are likely to give rise to new types of coordination behavior and structures. Phosphonocarboxylates can be considered as the link between the traditional open-framework structures and the recently discovered metal–organic framework compounds. The difference in the coordinating ability between the phosphonic acid and the carboxylic acid has been exploited fruitfully, resulting in a variety of interesting compounds.^{14,17–20} We have been intrigued by the possibility of combining the multiple coordination ability of the actinide elements with the flexible coordinating ability of the phosphonocarboxylate ligand. To this end, we have carried out reactions under hydrothermal conditions, employing thorium and uranium as model actinide elements. Our experiments have yielded three distinct products, $[\text{C}_4\text{N}_2\text{H}_{14}][(\text{UO}_2)_2(\text{O}_3\text{PCH}_2\text{COO})_2] \cdot \text{H}_2\text{O}$, **I**, $[\text{C}_4\text{N}_2\text{H}_{14}][(\text{UO}_2)_2(\text{C}_2\text{O}_4)(\text{O}_3\text{PCH}_2\text{COOH})_2]$, **II**, and $\text{Th}(\text{H}_2\text{O})_2(\text{O}_3\text{PCH}_2\text{COO})(\text{C}_2\text{O}_4)_{0.5} \cdot \text{H}_2\text{O}$, **III**. The structures of the compounds were formed by the connectivity involving the metal polyhedra and the phosphonoacetate/oxalate units. The close structural relationship between **I** and **III** prompted us to investigate the possibility of obtaining the uranium analogue of **III** via a solvent-free transformation reaction; solid state transformation studies of this nature, to the best of our knowledge, have been carried out for the first time. In this paper, we describe the synthesis, structure, and characterization of all the three phases.

Experimental Section

The uranium(VI) and thorium(IV) phosphonocarboxylates **I** and **III** were synthesized using hydrothermal methods. **II** was prepared by carrying out a solvent-free reaction. For the synthesis of **I**, uranyl acetate ($\text{UO}_2(\text{CH}_3\text{CO}_2)_2 \cdot 2\text{H}_2\text{O}$) (0.25 mmol, 0.106 g) was dispersed in 5 mL of distilled water. To this, phosphonoacetic acid (1.7 mmol, 0.242 g), oxalic acid (2.2 mmol, 0.278 g), and 1,4-diaminobutane (1,4-DAB) (0.92 mmol, 0.097 mL) were added with constant stirring, and the mixture was homogenized at room temperature. The reaction mixture was heated in a 23 mL PTFE-lined autoclave at 150 °C for 48 h. The autoclave was then cooled to room temperature. The initial pH of the mixture was 2.0 and there was no appreciable change in pH during the course of the reaction. Compound **I** can also be prepared without the use of oxalic acid in the synthesis mixture. For the synthesis of **II**, compound **I** (0.07 mmol, 0.064 g) was heated with solid oxalic acid (1 mmol, 0.126 g) at 150 °C for 48 h in a 23 mL PTFE-lined autoclave. Compound **II** was also obtained by grinding compound **I** and

oxalic acid in an agate mortar and pestle. Compound **III** was obtained by heating a mixture of $\text{Th}(\text{NO}_3)_4 \cdot 5\text{H}_2\text{O}$ (0.25 mmol, 0.144 g), phosphonoacetic acid (1.7 mmol, 0.242 g), $\text{H}_2\text{C}_2\text{O}_4$ (2.2 mmol, 0.278 g), 1,4-DAB (0.92 mmol, 0.097 mL), and distilled water (278 mmol, 5.0 mL) in a 23 mL Teflon-lined reaction vessel at 150 °C for 48 h. Pale-yellow plate-like crystals were obtained for compounds **I** and **II**, while colorless plate-like crystals were obtained for compound **III**. Yields: 73% based on uranium, 65% based on uranium, and 84% based on thorium, for **I**, **II**, and **III**, respectively. Compound **II** was synthesized by both the high-temperature solvent-free approach and the room-temperature mechanochemical route. The characterization studies of **II** were carried out on the product obtained by the high-temperature solvent-free method.

CHN analysis for compounds **I**, **II**, and **III** was carried out using a CHNS analyzer (ThermoFinnigan FLASH EA 1112 CHNS analyzer). Calcd. For **I**: C 10.41, H 2.17, N 3.04; found: C 9.67, H 2.03, N 2.98; Calcd. for **II**: C 12.26, H 2.04, N 2.86; found: C 12.16, H 1.92, N 2.72; Calcd. for **III**: C 7.71, H 1.7; found: C 7.55, H 1.67.

The powder X-ray diffraction (XRD) patterns were recorded on well-ground samples in the 2θ range 5–50° using Cu K α radiation (Philips X'pert Pro). The XRD patterns of the compounds **I–III** indicated that the products were pure and consistent with the XRD patterns simulated from the single crystal structure (see Supporting Information, Figure S1).

TGA studies have been carried out (Mettler-Toledo, TG850) in oxygen atmosphere (flow rate = 50 mL/min) in the temperature range 25–800 °C (heating rate = 5 °C/min) (Supporting Information, Figure S2). The TGA studies of **I** show a weight loss of ~1.7% between 90 and 200 °C, corresponding to the loss of lattice water (calcd 1.9%). Thereafter the compound loses weight in a series of small continuous steps between 200 and 700 °C. This weight loss may be attributed to the loss of the organic amine and the partial decomposition of the phosphonocarboxylate ligand (calcd 22.3%, obsd. 21.6%). The final decomposition product was identified by powder XRD to be a mixture of $\text{U}_3(\text{PO}_4)_4$ (JCPDS: 16-0225) and UP_2O_7 (JCPDS:16-0233). The TGA studies of **II** show a weight loss of ~17.8% over a broad temperature range of 100–400 °C. This corresponds to the loss of both the amine molecules and the oxalate moieties (calcd 18.2%). This is followed by another weight loss of ~9.98% in the region 600–800 °C, attributable to the partial decomposition of the phosphonocarboxylate ligand (calcd 12.1%). The final decomposition product was found to be poorly crystalline, with the majority of the XRD lines corresponding to the phase, UP_2O_7 (JCPDS:16-0233). In the case of compound **III**, the initial weight loss of 3.4% in the temperature range 30–95 °C corresponds to the loss of the lattice water molecule (calcd 3.9%). The second weight loss of 16.1% observed in the temperature range 100–350 °C corresponds to the loss of the coordinated water molecules (calcd 7.7%), and the decomposition of the oxalate moiety (calcd 9.4%). The final weight loss of 11.5% observed in the temperature range of 350–650 °C could be due to the partial decomposition of the phosphonocarboxylate ligand (calcd 12.4%). The calcined product was poorly crystalline, with a few of the XRD lines corresponding to the thorium phosphate phase, ThP_2O_7 (JCPDS: 17-0576).

IR spectroscopic studies were carried out in the range 400–4000 cm^{-1} using the KBr pellet method (Perkin-Elmer, SPECTRUM 1000) (Supporting Information, Figure S3). The infrared spectra of compounds **I** and **II** reveal the symmetric and antisymmetric stretches due to the UO_2^{2+} group in the regions 810–855 cm^{-1} and 907–916 cm^{-1} . For compound **III**, the Th–O stretches appears in the range 500–525 cm^{-1} . The peaks in the region 3530–3580 cm^{-1} can be attributed to the bound water molecules, while those in the region 3070–3185 cm^{-1} may be due to the lattice water molecules. The

(12) Clearfield, A. *Comments Inorg. Chem.* **1990**, *10*, 89.

(13) Chen, Z.; Zhou, Y.; Weng, L.; Yuan, C.; Zhao, D. *Chem. Asian J.* **2007**, *2*, 1549.

(14) Maeda, K. *Microporous Mesoporous Mater.* **2004**, *73*, 47.

(15) Schunk, S. A.; Schueth, F. *Mol. Sieves* **1998**, *1*, 229.

(16) Zhang, X.-M. *Eur. J. Inorg. Chem.* **2004**, *3*, 544.

(17) Zhang, X.-M.; Hou, J.-J.; Zhang, W.-X.; Chen, X.-M. *Inorg. Chem.* **2006**, *45*, 8120.

(18) Chen, Z.; Zhou, Y.; Weng, L.; Zhao, D. *Cryst. Growth. Des.* **2008**, *8*, 4045.

(19) Stock, N.; Karaghiosoff, K.; Bein, T. *Z. Anorg. Allg. Chem.* **2004**, *630*, 2535.

(20) Stock, N.; Frey, S. A.; Stucky, G. D.; Cheetham, A. K. *J. Chem. Soc., Dalton Trans.* **2000**, 4292.

stretching vibrations of the tetrahedral $-\text{CPO}_3$ groups are indicated by the presence of intense bands in the region $900\text{--}1100\text{ cm}^{-1}$, while the O--P--O bending vibrations are observable in the region $500\text{--}600\text{ cm}^{-1}$. The $\nu(\text{C=O})$ of the bound carboxylate groups are observed at $1350\text{--}1390\text{ cm}^{-1}$ (symm) and $1500\text{--}1545\text{ cm}^{-1}$, and the $-\text{CH}_2$ group vibrations are observed around 2900 cm^{-1} . In compound **I**, the $\nu(\text{C=O})$ of the unbound carboxylate group is observed between 1700 and 1715 cm^{-1} , and the vibrations due to the O--H in $-\text{COOH}$ are observed at $\sim 3100\text{ cm}^{-1}$. The various IR bands are consistent with those observed in other related compounds.¹

Room temperature solid-state photoluminescence studies were carried out on the powdered samples of compounds **I** and **II** (Perkin-Elmer, U.K. model no. LS55). The compounds were excited at 365 nm .

Single-Crystal Structure Determination. A suitable single crystal of each compound was carefully selected under a polarizing microscope and glued to a thin glass fiber. The single crystal diffraction data were collected on a Bruker AXS Smart Apex CCD diffractometer at room temperature (293 K). The X-ray generator was operated at 50 kV and 35 mA using $\text{Mo K}\alpha$ ($\lambda = 0.71073\text{ \AA}$) radiation. Data were collected with ω scans of width 0.3° . A total of 606 frames were collected in three different settings of φ ($0, 90,$ and 180°), keeping the sample-to-detector distance fixed at 6 cm and the detector position fixed at -25° . Pertinent experimental details of the structure determination of **I–III** are presented in Table 1.

The data were reduced using SAINTPLUS,²¹ and an empirical absorption correction was applied using the SADABS program.²² The crystal structure was solved and refined by direct methods using SHELXL-97 present in the WinGx suite of programs.²³ The hydrogen positions for the carbon atoms of the phosphonoacetate group (in **I** and **II**), the coordinated water oxygens (in **II**), and the amine molecule (in **I**) were placed in geometrically ideal positions and refined using the riding mode. The lattice water molecules in **I** and **II**, the amine molecules, the carbon atoms of the $-\text{CH}_2$ group, and the oxygen atoms of the $-\text{COOH}$ group in the phosphonoacetate ligand in **III** were found to be disordered. The location of hydrogen positions for the disordered water, phosphonocarboxylate, and amine molecules was not feasible, and only isotropic refinement was carried out. The last cycles of refinements included all the atomic positions, anisotropic thermal parameters for all the non-hydrogen atoms, and isotropic thermal parameters for all the hydrogen atoms. Full-matrix-least-squares structure refinement against $|F|^2$ was carried out using the WinGx suite of program.²³ CCDC 772574, 774427, 772575 contain the supplementary crystallographic data (CIF files) for the compounds **I**, **II**, and **III** respectively. The data can be obtained free of charge from The Cambridge Crystallographic Data Centre via www.ccdc.cam.ac.uk/data_request/cif.

Results

Structure of $[\text{C}_4\text{N}_2\text{H}_{14}][(\text{UO}_2)_2(\text{O}_3\text{PCH}_2\text{COO})_2] \cdot \text{H}_2\text{O}$, **I.** The asymmetric unit of **I** consists of 29 non-hydrogen atoms, of which two U atoms are crystallographically independent. Each uranium atom is connected to seven oxygen atoms and exhibits pentagonal bipyramidal geometry. The average U=O distance is 1.778 \AA , and the U--O_{eq} distances are in the range $2.264(9)\text{--}2.532(10)\text{ \AA}$

Table 1. Crystal Data and Structure Refinement Parameters for Compounds **I–III**^a

	I	II	III
empirical formula	$\text{C}_8\text{H}_{18}\text{N}_2\text{O}_{15}\text{P}_2\text{U}_2$	$\text{C}_5\text{NO}_9\text{PU}$	$\text{C}_3\text{H}_6\text{O}_{10}\text{PTH}$
formula weight	922.06	978.056	467.04
crystal system	triclinic	monoclinic	triclinic
space group	$P\bar{1}$ (no. 2)	$C2/m$ (no. 12)	$P\bar{1}$ (no. 2)
crystal size (mm)	$0.16 \times 0.14 \times 0.08$	$0.14 \times 0.12 \times 0.10$	$0.16 \times 0.12 \times 0.10$
a (\AA)	7.0758(3)	16.079(5)	6.9273(4)
b (\AA)	10.8016(8)	7.0030(15)	8.3531(3)
c (\AA)	14.8710(10)	10.228(3)	8.9612(3)
α (deg)	82.893(6)	90	101.263(3)
β (deg)	87.135(4)	104.34(3)	90.434(4)
γ (deg)	85.813(4)	90	111.414(4)
volume (\AA^3)	1123.88(12)	1115.8(5)	471.67(4)
Z	2	4	2
temperature (K)	293	293	293
ρ_{calcd} (g cm^{-3})	2.719	2.899	3.275
μ (mm^{-1})	14.601	14.726	16.017
wavelength (\AA)	0.71073	0.71073	0.71073
θ range (deg)	2.48 to 26.00	2.61 to 25.99	2.68 to 25.49
reflection collected	21515	2064	8286
unique reflections	4328	1120	1618
no. of parameters	262	108	152
goodness of fit	0.970	1.059	1.061
R index [$I > 2\sigma(I)$]	$R_1 = 0.0558$ $wR_2 = 0.1273$	$R_1 = 0.0488$ $wR_2 = 0.1063$	$R_1 = 0.0382$ $wR_2 = 0.1008$

^a $R_1 = \sum ||F_o| - |F_c|| / \sum |F_o|$; $wR_2 = \{ \sum w(F_o^2 - F_c^2)^2 / \sum w(F_o^2)^3 \}^{1/2}$. $w = 1 / [\rho^2(F_o^2) + (aP)^2 + bP]$. $P = [\max(F_o, 0) + 2(F_o)^2] / 3$, where $a = 0.0846$ and $b = 0.0000$ for **I**, $a = 0.0531$, $b = 12.8114$ for **II**, $a = 0.0799$ and $b = 0.0000$ for **III**.

(av. 2.38 \AA) (Table 2). The shorter uranyl distances (U=O) have been observed before by other researchers as well.^{1a,c,5c,24} The U(VI) sites are bound to two terminal axial oxygen atoms, [U(1)--O(1) , O(2) and U(2)--O(7) , O(8)], forming the uranyl (UO_2)²⁺ species. Three phosphonate oxygens, [U(1)--O(3) , O(4) , O(14) and U(2)--O(9) , O(10) , O(11)] and two carboxylate oxygens [U(1)--O(5) , O(6) and U(2)--O(12) , O(13)] from the phosphonoacetate ligands bind equatorially to the uranyl group, completing the pentagonal bipyramidal geometry around the uranium atom (Supporting Information, Figure S4). Each of the three oxygens of the phosphonate group coordinate in a monodentate fashion to only one uranium atom, which is generally referred to as a (111) connection.²⁵

The connectivity between the uranium and the μ_4 -coordinated phosphonoacetate units results in an anionic two-dimensional layer (Figure 1a). These layers are stacked one over the other along the a -axis in an $ABAB\dots$ fashion, as shown in Figure 1b. Charge compensation is achieved by the presence of protonated 1,4-diaminobutane molecules in between the layers. The interlamellar spaces also contain water molecules. The amine molecules participate in $\text{N--H}\cdots\text{O}$ type hydrogen bond interactions (Supporting Information, Table S2).

Structure of $[\text{C}_4\text{N}_2\text{H}_{14}][(\text{UO}_2)_2(\text{C}_2\text{O}_4)(\text{O}_3\text{PCH}_2\text{COOH})_2]$, **II.** The asymmetric unit of **II** consists of 15 non-hydrogen atoms, of which one uranium is crystallographically independent. The uranium atom is coordinated to seven oxygen atoms, and exhibits pentagonal bipyramidal geometry.

(21) SMART (V 5.628), SAINT (V 6.45a), XPREP and SADABS; Bruker AXS Inc.: Madison, WI, 2004.

(22) Sheldrick, G. M. SADABS Siemens Area Detector Absorption Correction Program; University of Göttingen: Göttingen, Germany, 1994.

(23) Farrugia, L. J. WinGx V 1.64.05, Crystallographic Program for Windows; 2003.

(24) (a) Borkowski, L. A.; Cahill, C. L. *Inorg. Chem.* **2003**, *42*, 7041. (b) Bharara, M. S.; Gordon, A. E. V. *Dalton Trans.* **2010**, *39*, 3557. (c) Giesting, P. A.; Porter, N. J.; Burns, P. C. Z. *Kristallogr.* **2006**, *221*, 252. (d) Burns, P. C.; Ewing, R. C.; Hawthorne, F. C. *Can. Mineral.* **1997**, *35*, 1551.

(25) Massiot, D.; Drumel, S.; Janvier, P.; Doeuiff, M. B.; Bujoli, B. *Chem. Mater.* **1997**, *9*, 6.

Table 2. Selected Bond Distances in Compounds I–III

bond	distance (Å)	bond	distance (Å)
Compound I ^a			
U(1)–O(1)	1.755(8)	P(2)–O(11)	1.526(10)
U(1)–O(2)	1.758(9)	P(2)–O(10)	1.544(10)
U(1)–O(3)	2.274(9)	P(2)–O(3)	1.553(10)
U(1)–O(4)	2.292(10)	P(2)–C(1)	1.805(15)
U(1)–O(14)	2.300(9)	O(4)–P(1)#3	1.526(10)
U(1)–O(5)	2.530(10)	O(5)–C(4)	1.256(16)
U(1)–O(6)	2.532(10)	O(6)–C(4)	1.262(16)
U(2)–O(7)	1.782(12)	O(11)–U(2)#3	2.330(9)
U(2)–O(8)	1.814(12)	O(12)–C(2)#2	1.279(16)
U(2)–O(9)	2.264(9)	O(13)–C(2)#2	1.233(16)
U(2)–O(10)	2.305(9)	C(1)–C(2)	1.531(19)
U(2)–O(11)#1	2.331(9)	C(2)–O(12)#2	1.279(16)
U(2)–O(12)	2.479(9)	N(1)–C(13)	1.45(2)
U(2)–O(13)	2.497(9)	N(2)–C(10)	1.47(2)
P(1)–O(14)	1.519(10)	C(10)–C(11)	1.49(2)
P(1)–O(9)	1.520(9)	C(11)–C(12)	1.46(2)
P(1)–O(4)#1	1.524(11)	C(13)–C(12)	1.48(3)
P(1)–C(3)	1.841(16)	C(3)–C(4)#4	1.493(19)
Compound II ^b			
U(1)–O(1)	1.769(9)	C(1)–C(3)#3	1.47(3)
U(1)–O(2)	1.799(13)	C(2)–O(5)#4	1.252(12)
U(1)–O(3)#1	2.297(13)	C(2)–C(2)#5	1.53(4)
U(1)–O(4)	2.317(9)	C(3)–O(7)	1.18(3)
U(1)–O(4)#2	2.317(9)	C(3)–O(6)	1.27(3)
U(1)–O(5)	2.495(9)	C(3)–O(7)#3	1.69(3)
U(1)–O(5)#2	2.495(9)	N(10)–C(10)#6	1.35(4)
P(1)–O(3)	1.512(13)	N(10)–C(10)	1.35(4)
P(1)–O(4)	1.520(9)	C(10)–C(11)#6	1.21(4)
P(1)–O(4)#3	1.520(9)	C(10)–C(11)	1.49(5)
P(1)–C(1)	1.83(2)	C(11)–C(10)#6	1.21(4)
O(3)–U(1)#1	2.297(13)	C(11)–C(11)#7	1.23(8)
O(5)–C(2)	1.252(12)	C(11)–C(11)#8	1.52(8)
Compound III ^c			
Th(1)–O(1)	2.296(8)	P(1)–C(1)#3	1.828(10)
Th(1)–O(3)	2.314(7)	O(2)–P(1)#2	1.524(8)
Th(1)–O(2)	2.315(8)	O(3)–P(1)#1	1.504(7)
Th(1)–O(4)	2.462(7)	O(5)–C(2)	1.257(13)
Th(1)–O(5)	2.515(7)	O(7)–C(3)	1.260(12)
Th(1)–O(6)	2.555(9)	O(8)–C(2)#4	1.256(14)
Th(1)–O(7)	2.564(8)	O(9)–C(3)	1.275(12)
Th(1)–O(8)	2.578(7)	C(3)–C(1)	1.492(13)
Th(1)–O(9)	2.602(8)	C(1)–P(1)#5	1.828(10)
P(1)–O(3)#1	1.504(7)	C(2)–O(8)#4	1.256(14)
P(1)–O(2)#2	1.524(8)	C(2)–C(2)#4	1.50(2)
P(1)–O(1)	1.533(8)		

^a Symmetry transformations used to generate equivalent atoms for I: #1 $x+1, y, z$ #2 $-x+1, -y+1, -z$ #3 $x-1, y, z$ #4 $-x+1, -y, -z+1$. ^b Symmetry transformations used to generate equivalent atoms for II: #1 $-x+3/2, -y+1/2, -z$ #2 $x, -y, z$ #3 $x, -y+1, z$ #4 $-x+1, y, -z-1$ #5 $-x+1, -y, -z-1$ #6 $x, -y-1, z$ #7 $-x+1, y, -z$ #8 $-x+1, -y-1, -z$. ^c Symmetry transformations used to generate equivalent atoms for III: #1 $-x+1, -y+2, -z$ #2 $-x, -y+2, -z$ #3 $x, y, z-1$ #4 $-x, -y+1, -z$ #5 $x, y, z+1$.

The average U=O distance is 1.782 Å, and the U–O_{eq} distances are in the range 2.297(13)–2.495(10) Å (av. 2.38 Å) (Table 2). Similar uranium–oxygen distances have been observed before.^{1a,c,5c,24} As in compound I, the U(VI) sites are bound to two terminal oxygen atoms, [O1, O2], giving rise to the uranyl (UO₂)²⁺ species. The pentagonal bipyramidal geometry is due to the bonding of three phosphonate oxygens from three phosphonoacetate ligands [O3, O4, #O4], and to two oxygens from the oxalate moiety [O5, #O5], along with the terminal uranyl oxygens (Supporting Information, Figure S4).

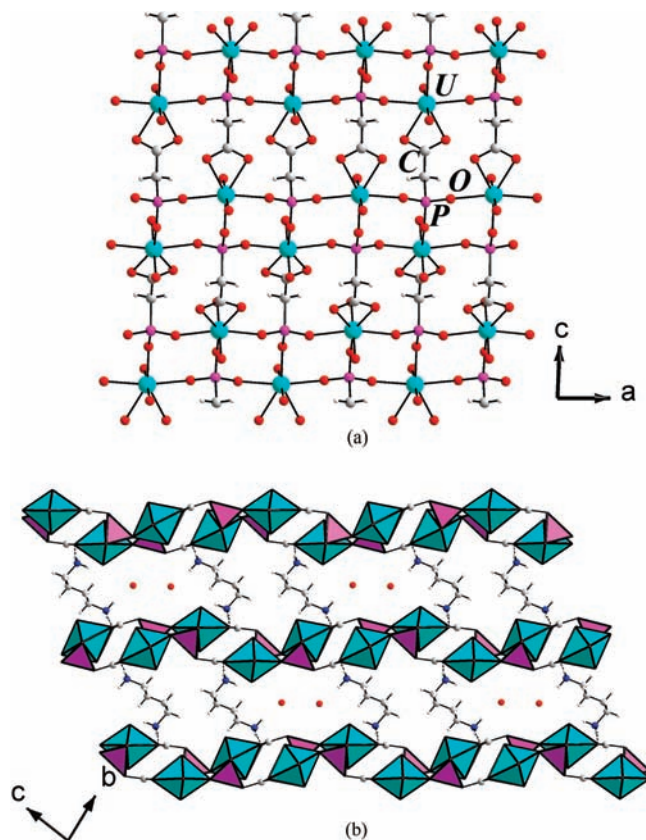


Figure 1. (a) View of the two-dimensional layer structure of [C₄N₂H₁₄]-[(UO₂)₂(O₃PCH₂COO)₂]·H₂O, I, along the *b*-axis. (b) The arrangement of the layers in the “*bc*” plane. The amine and lattice water molecules are located in the interlayer spaces. Dotted lines represent possible hydrogen bond interactions. (Cyan polyhedra: Uranium(VI) atoms in pentagonal bipyramidal geometry; Purple polyhedra: Phosphorus atoms of the phosphonoacetate ligand).

The connectivity between the uranyl group and the phosphonate oxygens of the phosphonoacetate ligand gives rise to a one-dimensional ladder-like arrangement. These ladders are then connected by oxalate bridges giving rise to an anionic layered structure (Figure 2a and Supporting Information, Figure S5). The non-bonded carboxylate oxygens of the phosphonoacetate project into the interlayer spaces (Figure 2b). The charge-compensating protonated 1,4-DAB molecules also occupy the interlayer spaces. The DAB molecules are disordered.

Structure of Th(H₂O)₂(O₃PCH₂COO)(C₂O₄)_{0.5}·H₂O, III. The asymmetric unit of III has 15 non-hydrogen atoms, of which one thorium is crystallographically independent. The thorium atom is coordinated to nine oxygen atoms and exhibits tricapped trigonal prism geometry, with an average Th–O bond distance of 2.467 Å (Table 2). The connectivity between the phosphonoacetate groups and the thorium atom results in a bonding similar to that observed in compound I. The central thorium atom is bound to three phosphonate oxygens, [O(1), O(2), O(3)] from three phosphonoacetate ligands, and to two carboxylate oxygens, [O(7), O(9)] from a fourth ligand. In addition, two water molecules [O(4), O(6)] are also bound to the central metal atom (Supporting Information, Figure S4).

The connectivity between thorium and phosphonoacetate gives rise to two-dimensional cationic layers along the *b*-axis (Figure 3a). These two-dimensional sheets are

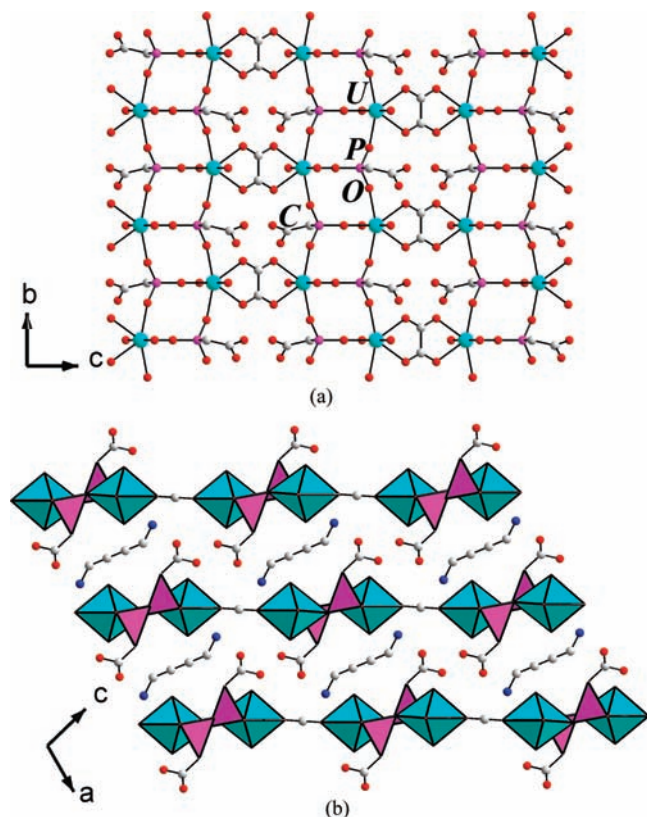


Figure 2. (a) View of the uranium phosphonoacetate-oxalate layers in $[\text{C}_4\text{N}_2\text{H}_{14}][(\text{UO}_2)_2(\text{C}_2\text{O}_4)(\text{O}_3\text{PCH}_2\text{COOH})_2]$, **II**, along the a -axis. (b) The arrangement of the layers in **II** in the “ ac ” plane. The disordered amine molecules are located in the interlayer spaces. Note that the carboxylate groups project into the interlamellar spaces. (Cyan polyhedra: Uranium(VI) atoms in pentagonal bipyramidal geometry; Purple polyhedra: Phosphorus atoms of the phosphonoacetate ligand).

bridged through the oxygen atoms of the oxalate moiety [O(5), O(8)] forming the three-dimensional structure. The thorium phosphonoacetate layers are stacked in an $AAA\dots$ fashion, pillared by the oxalate units (Figure 3b). This connectivity gives rise to one-dimensional channels of dimensions $10.83 \times 5.39 \text{ \AA}^2$ (longest atom–atom contact distance not including the van der Waals radii) along the c -axis (Supporting Information, Figure.S6). Extra-framework water molecules occupy these channels along with the water molecules coordinated to the thorium atom, which project into the channels. The calculated void space²⁶ in **II** is $\sim 9.1\%$.

Fluorescence Studies. The diffuse reflectance spectra of compounds **I** and **II** exhibit absorption bands in the visible region, between $350\text{--}500 \text{ cm}^{-1}$ (see Supporting Information, Figure S8). The bands in the $400\text{--}500 \text{ nm}$ region (centered at $\sim 420 \text{ nm}$) contain fine structures, and may be responsible for the pale yellow color of the compounds. The transitions may occur from the bonding orbitals to the non-bonding orbitals of uranium, which are generally forbidden.²⁷ Thus, the absorption intensity in the visible

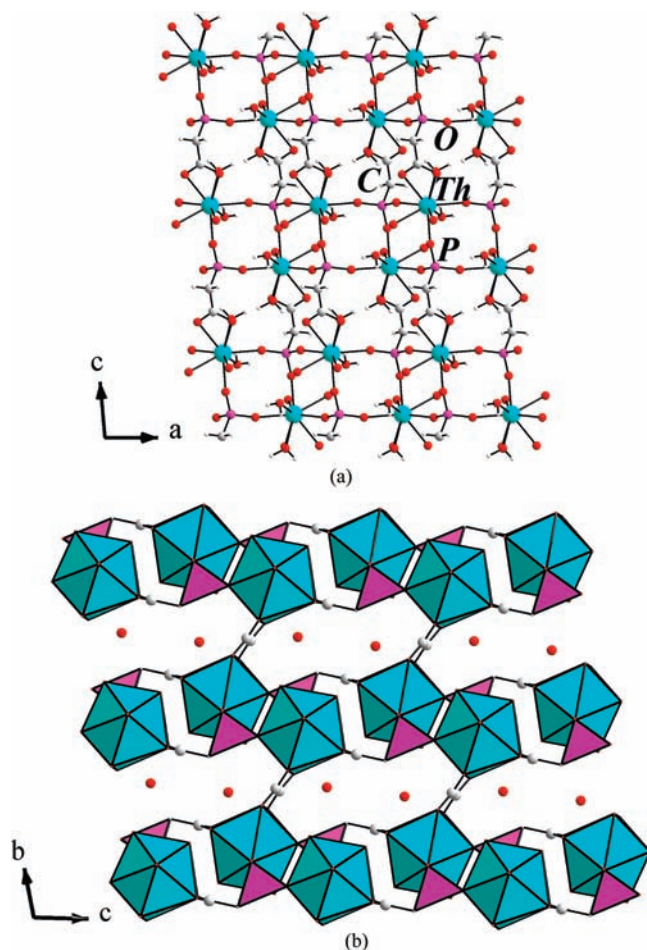


Figure 3. (a) View of the thorium phosphonoacetate layers in $\text{Th}(\text{H}_2\text{O})_2\text{-(O}_3\text{PCH}_2\text{COO})(\text{C}_2\text{O}_4)_{0.5}\cdot\text{H}_2\text{O}$, **III**, along the b -axis. Note the close similarity with the layer structure of **I**. (b) The three-dimensional structure of **III**. Note that the layers are connected by the oxalate units. The lattice water molecules are disordered and located in the channels. (Cyan polyhedra: Thorium(IV) atoms in tricapped trigonal prism geometry; Purple polyhedra: Phosphorus atoms of the phosphonoacetate ligand).

region for these compounds appear low. Fluorescence studies were carried out on compounds **I** and **II** using an excitation wavelength of 365 nm . A five-peak spectrum characteristic of compounds containing the uranyl ion^{5c,28} was obtained for both the compounds (Figure 4). Compound **II** exhibits a slight red-shift along with lesser intensity for the emission bands as compared to **I**. It is likely that the non-bonded carboxylate groups in **II** can participate in stronger H-bonds involving the amine molecules, which could be responsible for a drop in intensity in the emission spectrum of **II** as compared to **I**. Compound **III** exhibits no emission as neither Th^{4+} ($5f^0$) nor the ligand (phosphonoacetate) have absorption bands in this region.²⁹

Discussion

Of the three compounds prepared in the present study, compounds **I** and **III** were prepared hydrothermally, whereas

(26) Spek, A. L. *Platon: A Multi-purpose Crystallographic Tool*; Utrecht University: Utrecht, The Netherlands, 2001.

(27) (a) Huang, J.; Wang, X.; Jacobson, A. J. *J. Mater. Chem.* **2003**, *13*, 191. (b) Dai, S.; Shin, Y. S.; Toth, L. M.; Barnes, C. E. *Inorg. Chem.* **1997**, *36*, 4900. (c) Volkovich, V. A.; Griffiths, T. R.; Fray, D. J.; Thield, R. C. *Phys. Chem. Chem. Phys.* **2001**, *3*, 5182. (d) Burrows, H. D.; Kemp, T. J. *Chem. Soc. Rev.* **1974**, *3*, 139.

(28) (a) Almond, P. M.; Talley, C. E.; Bean, A. C.; Peper, S. M.; Albrecht-Schmitt, T. E. *J. Solid State Chem.*, **2000**, *154*, 635.

(29) (a) Blasse, G.; Grabmaier, B. C. *Luminescent Materials*; Springer-Verlag: New York, 1994; (b) Denning, R. G.; Norris, J. O. W.; Short, I. G.; Snellgrove, T. R.; Woodward, D. R. *Lanthanide and Actinide Chemistry and Spectroscopy*; Edelstein, N. M., Ed.; ACS Symposium Series 131; American Chemical Society: Washington, DC, 1980.

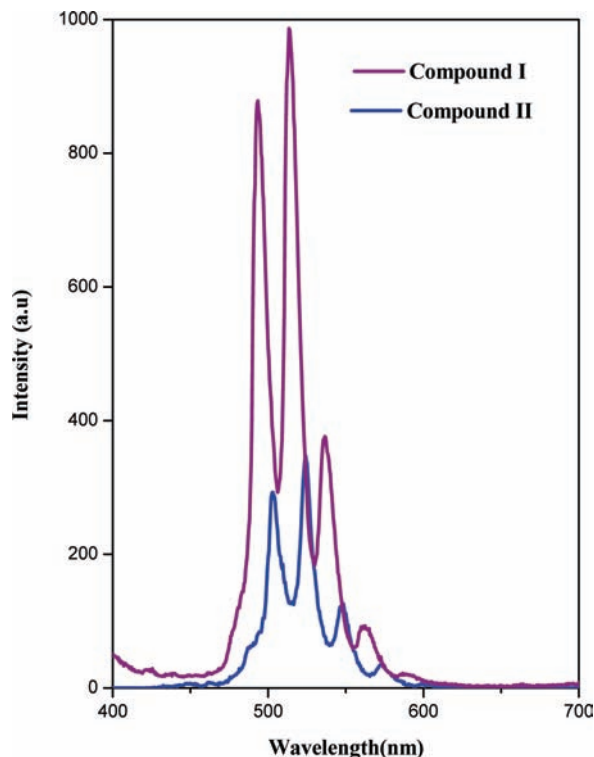


Figure 4. Emission spectra for compounds **I** and **II** via uranyl excitation at 365 nm.

compound **II** was synthesized using a solvent-free approach. Compound **II** can also be prepared by a mechanochemical (grinding) route at room temperature from **I**. The syntheses of the compounds **I** and **III** were carried out employing an organic amine (1,4-DAB), which was found to be part of the structure of **I**. In the case of compound **III**, the 1,4-DAB was not incorporated in the final structure. Our efforts to prepare compound **III** in the absence of 1,4-DAB were not successful. It is, therefore, possible that the amine (1,4-DAB) performs the roles of deprotonating the acid and maintaining the reaction pH during the synthesis of **III**. The deprotonating as well as the secondary role of amine molecules have been observed in the synthesis of many open-framework compounds.³⁰ It may be noted that the 1,4-diaminobutane molecules are also present in the structure of **II**, which can be prepared either at room temperature (by solid-state grinding) or at 150 °C (in a closed vessel). The 1,4-DAB molecules perform a templating role in both the structures of **I** and **II**. They also serve as charge-balancing counterions. The preparation of **II** from **I**, in a way, is reminiscent of the topotactic reactions, which are well established in solid state chemistry.³¹ Compounds **I** and **III** were obtained employing conventional

hydrothermal routes, whereas compound **II** was obtained as a product of transformation of **I** via a solvent-free method. The synthesis of open-framework compounds without employing any solvent molecules has been explored previously.³² This approach may have advantages as the possible influence of the solvent molecules on the formation of a particular framework structure can be avoided. In addition, the solvent-free approach involves lower pressures (because of the absence of any solvents) during the reaction, and may be safer for the synthesis of framework solids. Thus, this approach is, in a way, similar to the ionic liquid routes introduced recently for the preparation of many open-framework compounds.³³ During the present synthesis, the oxalic acid has a low melting point (101.5 °C), which helps in the formation of a flux at the reaction temperature of 150 °C. The transformation reaction was, however, not successful in the presence of water as the solvent. We observed that the oxalic acid dissolved in water, and compound **I** was recrystallized during the experiments.

Structurally all the compounds are related, having connectivities involving the metal polyhedra and the phosphonacetate units (**I**) and the oxalate, phosphonacetate units (**II** and **III**). The observation of ladder-like chain units in all the compounds is interesting as such units have been postulated to be one of the important building units in the assembly of structures of higher dimensionality.³⁴ Compounds **I** and **II** exhibit significant differences in connectivity. In **II**, the ladders are connected by oxalate units, whereas in **I**, the connectivity is through the carboxylate unit. Both **I** and **II** possess two-dimensional anionic layered structures, and the interlayer spaces are occupied by the protonated amine molecules. Compound **III**, on the other hand, possesses a 3D structure in which the thorium phosphonocarboxylate layers are connected by oxalate units forming a pillared layered arrangement. Thus, structurally, **I** and **III** appear to have a closer similarity as the layers have comparable connectivity. The layers in **I** are anionic, whereas the layers in **III** are cationic (Supporting Information, Figure S9). The charges are balanced by the protonated organic amine in **I** and by the oxalate units in **III**. It may be noted that oxalic acid has been used during the preparation in all the three cases (see Experimental Section), but we could obtain the three-dimensional compound with oxalates bridging the hybrid layer only in **III**. It is likely that the $(\text{UO}_2)^{2+}$ units with the apical terminal oxygens would have subtly influenced the formation of two-dimensional structures in **I** and **II**. Since the layers in compounds **I** and **III** appear to be comparable, we can examine the lattice parameters of the two compounds. Thus, the presence of the amine molecules (atom–atom contact length not including the van der Waals radii: 5.91 Å) in the interlayer spaces is reflected in the increased “c” lattice parameter of **I** (14.87 Å) as compared to **III** (8.96 Å). The layers in **III** are, however, bound by the oxalate units in the “b” direction. The oxalate units (size = 2.32 Å) are smaller than the organic amine molecules (size = 5.97 Å), and hence the decrease in the “b” lattice parameter of **III** matches reasonably well.

(30) (a) Natarajan, S. J. *Solid State Chem.* **1998**, *139*, 200. (b) Harrison, W. T. A.; Dussack, L. L.; Jacobson, A. J. *J. Solid State Chem.* **1996**, *125*, 234. (c) Mandal, S.; Natarajan, S. *Chem.—Eur. J.* **2007**, *13*, 968.

(31) (a) Rao, C. N. R.; Gopalakrishnan, J. *New Directions in Solid State Chemistry: Structure, Synthesis, Properties, Reactivity, and Material Design*; Cambridge Univ. Press: Cambridge, U.K., 1986. (b) West, A. R. *Solid State Chemistry and its Applications*; John Wiley and Sons: Chichester, U.K., 1984.

(32) (a) Lethbridge, Z. A. D.; Smith, M. J.; Tiwary, S. K.; Harrison, A.; Lightfoot, P. *Inorg. Chem.* **2004**, *43*, 11. (b) Lin, Z.; Dehnen, S. *J. Solid State Chem.* **2009**, *182*, 3143. (c) Lin, Z.; Nayek, H. P.; Dehnen, S. *Inorg. Chem.* **2009**, *48*, 3517. (d) Lin, Z.; Nayek, H. P.; Dehnen, S. *Microporous Mesoporous Mater.* **2009**, *126*, 95. (e) Lin, Z.-E.; Fan, W.; Gao, F.; Chino, N.; Yokoi, T.; Okubo, T. *Cryst. Growth. Des.* **2006**, *6*, 2435.

(33) (a) Parnham, E. R.; Morris, R. E. *Acc. Chem. Res.* **2007**, *40*, 1005. (b) Morris, R. E. *Chem. Commun.* **2009**, *21*, 2990. (c) Morris, R. E. *Stud. Surf. Sci. Catal.* **2008**, *174A*, 33 (Zeolites and Related Materials).

(34) (a) Ayi, A. A.; Choudhury, A.; Natarajan, S.; Neeraj, S.; Rao, C. N. R. *J. Mater. Chem.* **2001**, *11*, 1181. (b) Rao, C. N. R.; Natarajan, S.; Choudhury, A.; Neeraj, S.; Ayi, A. A. *Acc. Chem. Res.* **2001**, *34*, 80.

Transformation Studies. Transformation studies on low-dimensional compounds can provide pointers to the formation of structures of higher dimensionality.³⁴ During the present study, our synthetic efforts did not result in a three-dimensional uranium phosphonoacetate-oxalate under the experimental conditions (hydrothermal methods). This prompted us to explore the possibility of synthesizing a three-dimensional structure by carrying out transformation reactions using compound **I**, under suitable conditions. To this end, we carried out reactions between compound **I** and oxalic acid at 150 °C for 2 days in a 23 mL PTFE-lined autoclave without the use of any additional solvent molecules (solvent-free approach). Our studies yielded a new layered uranium phosphonoacetate-oxalate, **II**. Since compound **II** was prepared from **I** by solid state reactions at 150 °C, we wanted to explore the formation of **II** by other methods such as a simple solid state mechanochemical route. It may be noted that the solid state transformation of one phase to another by the mechanochemical route (grinding) has been elegantly established in organic solid state chemistry.³⁵ Such mechanochemical reactions have also been attempted in the preparation of metal–organic framework compounds recently.³⁶ The solid–state mechanochemical studies of the amine–templated open-framework compounds, however, have not been explored fully. A study of this nature could help in understanding how the transformation proceeds along with the possibility of exploring the formation of any intermediate phases, as the reactions are carried out at room temperature. In the present study, we have performed two sets of experiments. In one set, the formation of compound **II** from **I** was investigated as a function of time at 150 °C in an autoclave. In another set, we have performed a simple mechanochemical study (grinding) at room temperature. It is of interest to note that we have been able to synthesize the same compound with the same formula (compound **II**) by two independent procedures.

Compound **I** (0.07 mmol, 0.064 g) was mixed thoroughly with oxalic acid (1 mmol, 0.126 g), and heated at 150 °C in a 23 mL PTFE-lined autoclave for varying periods of time. The products, at different time intervals, were analyzed using powder XRD studies (Figure 5a). As can be noted, an unidentified phase, [*], forms initially along with the compound **II**. The unidentified phase persists for up to ~8 h, after which it vanishes. A closer examination of the powder XRD patterns suggests the possibility of the formation of a pillared layered structure closely resembling that of **III**.

It occurred to us that we could study and possibly isolate the intermediate by carrying out the reaction at a lower temperature. For this purpose, we took compound **I** (1 mmol, 0.126 g) and oxalic acid (1 mmol, 0.126 g), and employed the mechanochemical route at room temperature (Figure 5b). Surprisingly, we observed the formation

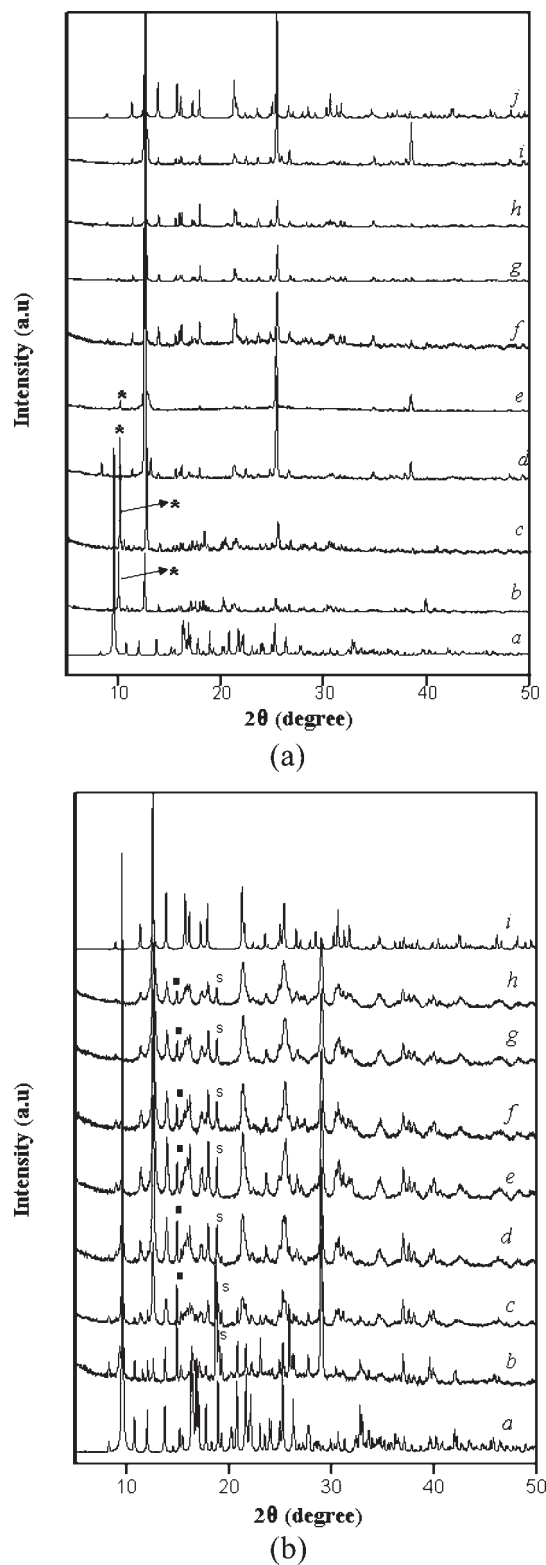


Figure 5. (a) Powder XRD patterns as a function of time during the transformation reaction of $[\text{C}_4\text{N}_2\text{H}_{14}][(\text{UO}_2)_2(\text{O}_3\text{PCH}_2\text{COO})_2] \cdot \text{H}_2\text{O}$, **I**, at 150 °C. (a) simulated pattern of **I**; Experimental pattern of **I** + oxalic acid: (b) after 2 h, (c) after 4 h, (d) after 6 h, (e) after 8 h, (f) after 12 h, (g) after 24 h, (h) after 36 h, (i) after 48 h (j) simulated pattern of compound **II**. ([*] denotes unidentified phase). (b) The powder XRD patterns as a function of time during the transformation reaction of $[\text{C}_4\text{N}_2\text{H}_{14}][(\text{UO}_2)_2(\text{O}_3\text{PCH}_2\text{COO})_2] \cdot \text{H}_2\text{O}$, **I**, by the mechanochemical route (grinding) at room temperature (a) simulated pattern of **I**; Experimental pattern of **I** + oxalic acid: (b) after 10 min, (c) after 1 h, (d) after 2 h, (e) after 3 h, (f) after 4 h, (g) after 5 h, (h) after 6 h, (i) simulated pattern of compound **II**. (■) denotes unidentified phase, s denotes source phase-compound **I**.

(35) (a) Desiraju, G. R. *Crystal Engineering: The Design of Organic Solids*; Elsevier: Amsterdam, The Netherlands, 1989; (b) Braga, D.; Grepioni, F. *Angew. Chem., Int. Ed.* **2004**, *43*, 4002. (c) Gao, X.; Friscic, T.; MacGillivray, L. R. *Angew. Chem., Int. Ed.* **2004**, *43*, 232. (d) Kaupp, G. *CrystEngComm* **2003**, *5*, 117. (e) Kaupp, G. *CrystEngComm* **2009**, *11*, 388. (f) Trask, A. V.; Jones, W. *Top. Curr. Chem.* **2005**, *254*, 41 (Organic Solid State Reactions). (g) Jones, W. *Org. Mol. Solids* **1997**, *149*. (h) Nakamatsu, S.; Toyota, S.; Jones, W. *Chem. Commun.* **2005**, *30*, 3808.

(36) (a) Friscic, T.; Reid, D. G.; Halasz, I.; Stein, R. S.; Dinnebier, R. E.; Duer, M. J. *Angew. Chem., Int. Ed.* **2010**, *49*, 712. (b) Braga, D.; Polito, M.; Dichiarante, E.; Rubini, K.; Grepioni, F. *Chem. Commun.* **2007**, 1594.

of compound **II** almost immediately. We also observed the formation of a completely new unidentified phase, [■], along with compound **II**. Although the product phase forms completely by ~4 h, the XRD patterns showed the presence of minor quantities of the unidentified phase, [■], as well as that of the source, *s* (compound **I**), even after grinding for 6 h.

The present transformation studies of compound **I** suggest that the transformation proceeds via two independent pathways. At 150 °C, it is likely that the oxalate moiety finds a way to bind with the uranium centers along with the phosphonoacetate molecules initially. This binding would generate considerable strain on the uranium center, which leads to the breaking up of the intermediate to recrystallize compound **II**.

Transformation studies carried out on amine-templated open-framework phosphates have provided interesting clues.³⁴ Studies of this nature are important as our understanding of the formation of amine-templated open-framework compounds is still not adequate. The present studies employing two different approaches establish the reactive nature of **I**. The studies presented in this paper are preliminary in nature, and more experiments are required, preferably, employing *in situ* synchrotron based investigations. The synchrotron based studies have helped in formulating many intermediates and pathways during the synthesis of open-framework compounds.³⁷

(37) (a) Loiseau, T.; Walton, R. I.; Francis, R. J.; O'Hare, D.; Ferey, G. *J. Fluorine Chem.* **2000**, *101*, 181. (b) Loiseau, T.; Beitone, L.; Millange, F.; Taulelle, F.; O'Hare, D.; Ferey, G. *J. Phys. Chem. B* **2004**, *108*, 20020. (c) Miller, S. R.; Lear, E.; Gonzalez, J.; Slawin, A. M. Z.; Wright, P. A.; Guillou, N.; Ferey, G. *Dalton Trans.* **2005**, *20*, 3319. (d) Volkringer, C.; Loiseau, T.; Guillou, N.; Ferey, G.; Haouas, M.; Taulelle, F.; Audebrand, N.; Margiolaki, I.; Popov, D.; Burghammer, M.; Riekel, C. *Cryst. Growth Des.* **2009**, *9*, 2927.

Such studies would also be required for the present compounds to evaluate and understand both the mechanisms better.

Conclusions

The synthesis, structure and transformation studies on a family of actinide element containing compounds have been accomplished. Compound **II** has been synthesized in a solvent-free route. In addition, compound **I** was found to undergo a solid-state transformation to give rise to **II**. The observation of closely related structures in the actinide family suggests that this area would offer much scope for further investigation. The formation of oxalate hybrids using the phosphonocarboxylate ligand is a new approach in the synthesis of multicomponent hybrid compounds. Further work is presently underway to investigate other related phosphonocarboxylates.

Acknowledgment. S.N thanks the Department of Science and Technology (DST) and the Council of Scientific and Industrial Research (CSIR), Government of India, for the award of a research grant. S.N also thanks the Department of Science and Technology (DST), Government of India, for the award of a RAMANNA fellowship. The authors thank Mr. Saikat Sen for helpful discussions on crystallographic details.

Supporting Information Available: Selected bond angles for compounds **I**, **II**, and **III**; observed hydrogen bond interactions in compound **I**; Powder XRD patterns, IR spectra, TGA curves for compounds **I**, **II**, and **III**; UV-Vis spectra for compounds **I** and **II**; additional structure drawings. This material is available free of charge via the Internet at <http://pubs.acs.org>.